



**HAL**  
open science

## Measurements of the water vapor continuum absorption by OFCEAS at 3.50 $\mu\text{m}$ and 2.32 $\mu\text{m}$

H Fleurbaey, R Grilli, Didier Mondelain, A Campargue

► **To cite this version:**

H Fleurbaey, R Grilli, Didier Mondelain, A Campargue. Measurements of the water vapor continuum absorption by OFCEAS at 3.50  $\mu\text{m}$  and 2.32  $\mu\text{m}$ . *Journal of Quantitative Spectroscopy and Radiative Transfer*, 2022, 278, pp.108004. 10.1016/j.jqsrt.2021.108004 . hal-03854932

**HAL Id: hal-03854932**

**<https://hal.science/hal-03854932>**

Submitted on 17 Nov 2022

**HAL** is a multi-disciplinary open access archive for the deposit and dissemination of scientific research documents, whether they are published or not. The documents may come from teaching and research institutions in France or abroad, or from public or private research centers.

L'archive ouverte pluridisciplinaire **HAL**, est destinée au dépôt et à la diffusion de documents scientifiques de niveau recherche, publiés ou non, émanant des établissements d'enseignement et de recherche français ou étrangers, des laboratoires publics ou privés.

1                   **Measurements of the water vapor continuum absorption**  
2                   **by OFCEAS at 3.50  $\mu\text{m}$  and 2.32  $\mu\text{m}$**

3  
4  
5                   H. Fleurbaey <sup>1</sup>, R. Grilli <sup>2</sup>, D. Mondelain <sup>1</sup>, A. Campargue <sup>1\*</sup>

6                   <sup>1</sup> *Univ. Grenoble Alpes, CNRS, LIPhy, 38000 Grenoble, France*

7                   <sup>2</sup> *Univ. Grenoble Alpes, CNRS, IRD, Grenoble INP, IGE, 38000 Grenoble, France*

8  
9  
10  
11  
12  
13  
14  
15  
16  
17  
18  
19  
20  
21  
22  
23  
24  
25  
26  
27  
28  
29  
30  
31                   **Key words**

32                   Water vapor; continuum absorption; MT\_CKD model; OFCEAS; transparency window;  
33                   atmosphere

- 34  
35                   • *Corresponding author: Alain Campargue (Alain.Campargue@univ-grenoble-alpes.fr)*  
36

## Abstract

37  
38  
39  
40  
41  
42  
43  
44  
45  
46  
47  
48  
49  
50  
51  
52  
53  
54  
55  
56

Measurements of the water vapor absorption cross-sections at two spectral points of the 2.1  $\mu\text{m}$  and 4.0  $\mu\text{m}$  transparency windows are performed by optical feedback cavity enhanced absorption spectroscopy (OFCEAS).

The self-continuum cross-section,  $C_S$ , is measured for temperature values of 30 and 47  $^{\circ}\text{C}$  (303 and 320 K) at the 2853  $\text{cm}^{-1}$  spectral point, corresponding to the lowest opacity region of the 4.0  $\mu\text{m}$  transparency window. The  $C_S$  values derived from the pressure squared dependence of the self-continuum, are found consistent with previous CEAS measurements in the considered window but significantly smaller than measurements by Fourier transform spectroscopy (FTS). The  $C_S$  temperature dependence is discussed in relation with FTS measurements at high temperature.

Foreign-continuum cross-sections,  $C_F$ , are newly obtained from OFCEAS spectra of moist air in flow regime at the 4302  $\text{cm}^{-1}$  spectral point of the low energy edge of the 2.1  $\mu\text{m}$  window. After subtraction of the monomer and self-continuum contributions,  $C_F$  values are derived from the linear variation of the foreign-continuum absorption with the product of the water vapor and air partial pressure. The measurements were performed for temperature values of 34 and 47  $^{\circ}\text{C}$  (307 and 320 K) and no significant temperature variation is evidenced. The present  $C_F$  value at 4302  $\text{cm}^{-1}$  is gathered with previous CEAS measurements at seven spectral points of the 2.1  $\mu\text{m}$  window. This consistent set of  $C_F$  values is used to derive from a polynomial fit, the empirical frequency dependence of  $C_F(\nu)$  over the 4250-5000  $\text{cm}^{-1}$  range. Overall, the semi-empirical MT\_CKD\_3.5 values of  $C_F$  are significantly underestimated in the centre of the considered window.

## 57 1. Introduction

58 Water vapor is the first greenhouse gas of our atmosphere. Its absorption represents between 50 and 70  
59 % of the incoming solar light. The absorption spectrum of water vapor consists of narrow absorption  
60 lines due to transition between ro-vibrational levels of the water molecule and a more featureless  
61 continuum whose interpretation remains a major controversy in molecular spectroscopy [1]. The water  
62 spectrum is organized in bands of strong absorption, interspersed with a number of more transparent  
63 “windows”. Although its amplitude is smaller in the windows, the relative importance of the continuum  
64 is much higher than in the band regions where the line absorption generally dominates.

65 The insufficient knowledge of the water continuum in the near infrared transparency windows makes it  
66 an important source of uncertainty for the radiative budget of the Earth’s atmosphere. As a result of the  
67 lack of accurate experimental data, the semi-empirical MT\_CKD model [2-4] is generally implemented  
68 in atmospheric radiative transfer codes. This model uses an empirical line shape modeling with sub-  
69 Lorentzian far wings and a *weak interaction* term between a water vapor molecule and another molecule  
70 for the intermediate wings. The parameters of this profile are then fitted to few laboratory or field  
71 measurements available mostly in the mid infrared.

72 Indeed, the quantitative determination of weak absorption continua is generally challenging by  
73 transmission spectroscopy (like Fourier transform spectroscopy (FTS)) as the continuum shows up as a  
74 small decrease of the transmitted spectrum baseline. The challenge is made even more difficult in the  
75 case of water vapor because of possible surface effects on the optics of the experimental setup. During  
76 the last decade, large experimental efforts have been performed to complete the pioneer works of Burch  
77 [5-7] in the transparency windows. FTS allowed for large spectral coverage [8-10] and provided self-  
78 continuum cross-sections significantly higher than the generally adopted MT\_CKD values in the 4.0,  
79 2.1 and 1.6  $\mu\text{m}$  windows. These FTS measurements were not confirmed by our recent series of  
80 experiments using cavity enhanced absorption spectroscopy (CEAS) [11-18], namely cavity ring down  
81 spectroscopy (CRDS) and optical feedback–cavity enhanced absorption spectroscopy (OF-CEAS).  
82 These CEAS measurements, supported by a clear pressure squared dependence of the continuum  
83 absorption, have been recently used to constrain the MT\_CKD self-continuum in the 4.0, 2.1, 1.6 and  
84 1.25  $\mu\text{m}$  windows.

85 In the case of the foreign-continuum arising from interactions between water molecules and molecular  
86 oxygen and nitrogen, experimental data are even more scarce in particular at room temperature [20].  
87 Regarding the transparency windows, cross-sections provided by FTS [21-23] in the mid-IR windows  
88 and by cavity ring down spectroscopy (CRDS) in the 2.1  $\mu\text{m}$  window [16] have led to a significant  
89 increase of the MT\_CKD foreign-continuum since the 2.8 version [3].

90 The temperature dependence of the self- and foreign-continua is of importance for atmospheric  
91 applications. The self-continuum is known to have a strong negative dependence around room  
92 temperature while the foreign-continuum is believed to be much less sensitive to the temperature. Note  
93 that the temperature dependence may help to discriminate different processes responsible of the

94 continuum: far wings of the rovibrational lines, “water dimers” – and other bimolecular complexes, such  
 95 as O<sub>2</sub>-H<sub>2</sub>O and N<sub>2</sub>-H<sub>2</sub>O, and collision-induced absorption (CIA).

96 The present work is a further step in our experimental investigation of the water self- and foreign-  
 97 continua by CEAS. While the FTS technique allowed for wide spectral coverage, laser based techniques  
 98 are inherently more sensitive but generally limited to narrow spectral intervals depending of the  
 99 availability of laser sources. Here, we report on new OFCEAS self-continuum cross-section,  $C_S$ , at 30  
 100 and 47 °C at the 2853 cm<sup>-1</sup> spectral point in the center of the 4.0 μm transparency window and foreign-  
 101 continuum cross-sections,  $C_F$ , at the 4302 cm<sup>-1</sup> spectral point of the low energy edge of the 2.1 μm  
 102 window at 34 and 47 °C. In the following part 2, we will present the experimental procedure and data  
 103 acquisition adopted for the two series of measurements. Parts 3 and 4 are devoted to the retrievals of the  
 104 values of  $C_S$  at 2853 cm<sup>-1</sup> and  $C_F$  at 4302 cm<sup>-1</sup>, respectively and include a discussion of the comparison  
 105 with literature data and of the temperature dependence. For the convenience of the reader, we have  
 106 gathered in **Table 1**, the previous and present CEAS measurements of  $C_S$  in the 4.0 μm window and  $C_F$   
 107 in the 2.1 μm window.

108 **Table 1.** Summary of the CEAS measurements of self-continuum cross-sections,  $C_S$ , in the 4.0  
 109 μm window and foreign-continuum cross-sections,  $C_F$ , in the 2.1 μm window. Number in parenthesis  
 110 correspond to 1 σ uncertainty in units of the last digit.

Window Approx. center	Spectral point (cm <sup>-1</sup> )	$T(K)$	$C_S$ (10 <sup>-23</sup> cm <sup>2</sup> molecule <sup>-1</sup> atm <sup>-1</sup> )	Reference
2700 cm <sup>-1</sup> (4.0 μm)	2283 (4.38 μm)	296.15	1.26(6) <sup>a</sup>	<i>Campargue et al. 2016 [13]</i>
		301.15	1.18(6) <sup>a</sup>	
		312.15	0.88(4) <sup>a</sup>	
	2491 (4.014 μm)	297.3	0.41(3)	<i>Richard et al. 2017 [14]</i>
		312.3	0.305(43)	
		325.6	0.260(37)	
	<b>2853 (3.5 μm)</b>	<b>303.15</b>	<b>0.585(42)</b>	<b><i>This work</i></b>
		<b>320.15</b>	<b>0.428(39)</b>	
	3007 (3.3 μm)	298.15	1.96(39)	<i>Lechevallier et al. 2018 [15]</i>
		303.15	2.17(54)	
		308.15	1.83(46)	
		313.15	1.43(36)	
318.15		1.82(46)		
323.15		1.40(35)		
4700 cm <sup>-1</sup> (2.1 μm)			$C_F$ (10 <sup>-25</sup> cm <sup>2</sup> molecule <sup>-1</sup> atm <sup>-1</sup> )	
	4248.83	297	3.91(40) <sup>b</sup>	<i>Mondelain et al. 2015 [16]</i>
	4257.30		3.93(30) <sup>b</sup>	
	<b>4302</b>	<b>307.15</b>	<b>2.75(17)</b>	<b><i>This work</i></b>
		<b>320.15</b>	<b>2.60(18)</b>	
	4432.6	297	1.26(5)	<i>Vasilchenko et al. 2019 [17]</i>
	4436.3		1.15(5)	
4522.0	0.810(36)			
4724.1	0.444(43)			
4999.0	0.83(18)			

111 Notes

112 <sup>a</sup> Total uncertainty of 5% [13]. The (smaller) error bars given in Table 2 of Ref. [13] are limited to the fit  
 113 uncertainty

114 <sup>b</sup> Total uncertainty of 30% [16]. The (smaller) error bars given in Table 2 of Ref. [16] are limited to the fit  
 115 uncertainty.

116

## 117 2. Experimental setup

### 118 a. OF-CEAS spectrometers

119 OFCEAS is a high-sensitivity technique which relies on optical feedback to efficiently inject the probe  
120 laser into a high-finesse V-shaped cavity [24,25]. This technique has been used to measure water  
121 continua in other spectral regions [13-15, 18]. The reader is referred to [18] for a more detailed  
122 description. The use of a V-shaped cavity allows reinjecting part of the resonant intra-cavity field into  
123 the diode laser source. This optical feedback leads to laser emission width narrowing and a temporary  
124 locking of the laser frequency to the cavity mode, improving the efficiency of the cavity injection. Due  
125 to the fixed geometry of the cavity, the spectra have an intrinsically linear frequency scale with point  
126 spacing equal to the free spectral range (FSR). Both arms of the cavity have a nominally 40 cm length,  
127 corresponding to an FSR of 187.5 MHz. Applying a ramp on the diode laser current while keeping its  
128 temperature constant, spectra can be recorded over more than 100 cavity modes ( $\sim 0.6 \text{ cm}^{-1}$ ) at a rate of  
129 about 5 Hz. Transmission spectra are obtained by dividing the maximum output of the cavity at each  
130 mode by a reference photodiode signal, while a single ring down event is recorded at the end of each  
131 scan to retrieve the absolute absorption coefficient [26].

132 Two distinct OFCEAS spectrometers were used for the two spectral ranges covered in this work. In one  
133 setup, the probe laser was an interband cascade laser (ICL) tunable from  $2850 \text{ cm}^{-1}$  to  $2856 \text{ cm}^{-1}$ , and  
134 the baseline ring down time was  $13 \mu\text{s}$  corresponding to a mirror reflectivity of 99.990 %. The other  
135 setup used a distributed feedback (DFB) laser diode emitting around  $4300 \text{ cm}^{-1}$  and mirrors of  
136 reflectivity 99.997 % as determined from the baseline ring down time of  $45 \mu\text{s}$ .

137 For both setups, the cavity temperature was monitored with a thermistor of 0.3 K accuracy, and could  
138 be controlled between about 30 and 50 °C by heating bands regulated *via* a PID loop.

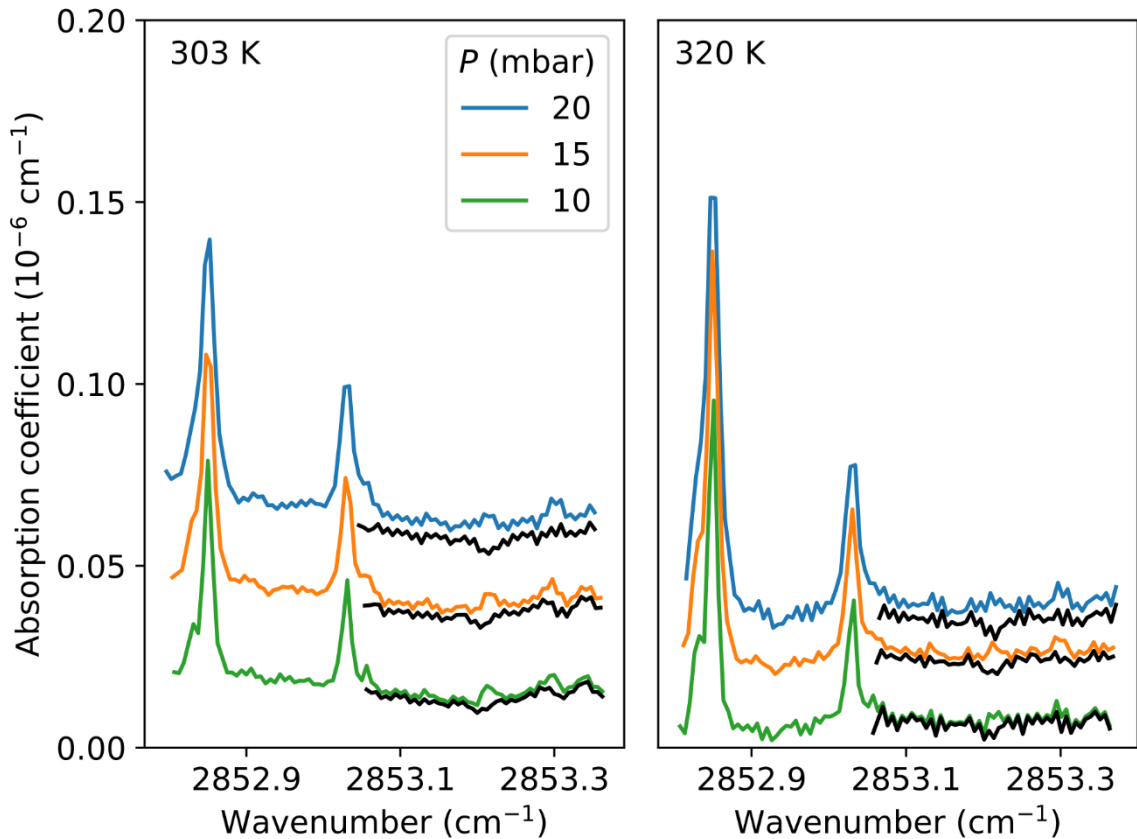
139 The baseline RMS noise was about  $1 \times 10^{-9} \text{ cm}^{-1}$  for the  $4302 \text{ cm}^{-1}$  setup. For the  $2853 \text{ cm}^{-1}$  setup, there  
140 was an additional, unexplained noise at higher temperature, so that the base line RMS noise ranged from  
141 about  $5 \times 10^{-9} \text{ cm}^{-1}$  at 30 °C, to  $1.6 \times 10^{-8} \text{ cm}^{-1}$  at 47 °C. In all cases, 100 spectra were averaged at each  
142 data point.

### 143 b. Self-continuum data acquisition

144 For the self-continuum measurements at  $2853 \text{ cm}^{-1}$ , a steel tank filled with deionised water was  
145 connected upstream of the cavity. A needle valve at the inlet of the cavity allowed adjusting the flow at  
146 a value of 3 to 4 sccm. At the outlet, an electrovalve was used to control the intra-cavity pressure, which  
147 was monitored with a Wika sensor (250 mbar full scale) calibrated against a MKS sensor (10 mbar  
148 range, 0.25 % accuracy).

149 A flow of water vapor through the cavity was initialized at a pressure of 20 mbar. Spectra were recorded  
150 at this pressure value, then the pressure was stepped down to approximately 5 mbar, before bringing it  
151 back up to 20 mbar. For each of those nine pressure steps, 100 spectra were averaged. This procedure  
152 was repeated for two temperature values: 30 °C and 47 °C. **Figure 1** shows spectra recorded at 10, 15

153 and 20 mbar, for both temperature values. The rapid increase of the continuum with pressure and the  
154 significant decrease with temperature are clearly observed.



155

156 **Figure 1:** Spectra recorded with pure water vapor at three pressure values, for two temperature conditions. Black  
157 lines denote the monomer-corrected spectra used to determine the self-continuum absorption. The constant term  
158 due to the empty cavity losses, obtained from the fit (see section 3a) was subtracted.

### 159 c. Foreign continuum data acquisition

160 A commercial humidity generator (from Omicron Technologies) was used to generate moist air for  
161 foreign continuum measurements. This generator is based on a temperature regulated membrane system  
162 to generate pure water vapor which is then mixed with the dry carrier gas (Alphagaz<sup>TM</sup>2 synthetic air  
163 from Air Liquide) with a proportional control solenoid valve with bypass to achieve the desired humidity  
164 level, monitored via the dew point temperature measured by a chilled mirror hygrometer (Michell  
165 Instruments). A flow controller and back pressure controller (both from Bronkhorst) regulated the gas  
166 flow (300 sccm) and the pressure (1045 mbar) in the exit. A part of this flow (about 10 sccm) was  
167 derived into the OFCEAS high-finesse cavity through another flow controller, while the intra-cavity  
168 pressure was stabilized to a value of 510 Torr (680 mbar) by a Bronkhorst pressure controller at the  
169 outlet.

170 The recording procedure was the following. First, dry nitrogen gas was flowed through the cavity at the  
171 same pressure value of 510 Torr to record the baseline cavity mirror losses. The gas source was then

172 switched to the moist air, and once the absorption in the cavity had reached a stable state (reflecting  
173 stability of the water mole fraction), 100 spectra were averaged before changing the water mole fraction  
174 set point to the next value. This procedure was repeated for two temperature values: 34 °C and 47 °C,  
175 and four water mole fraction values: 5000, 10000, 12500 and 15000 ppmv.

### 176 3. Self-continuum at 2853 cm<sup>-1</sup>

177 In a cell filled with pure water vapor, the total absorption coefficient can be expressed as the sum of  
178 three terms:

$$\alpha_{tot}(\nu, T) = \alpha_{cavity} + \alpha_{WML} + \alpha_{WCS} \quad (2)$$

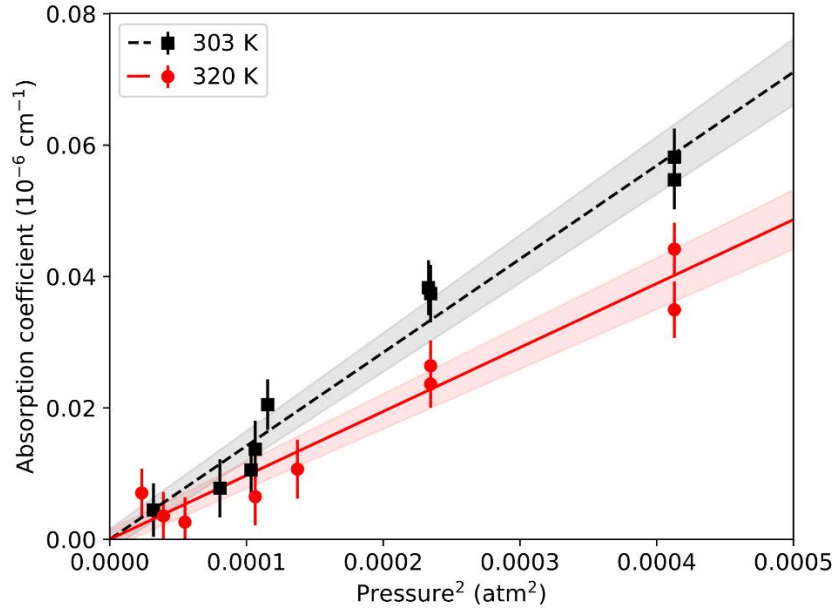
179 where  $\alpha_{cavity}$ ,  $\alpha_{WML}$ ,  $\alpha_{WCS}$  are the contributions due to the cavity, water vapor “monomer local lines”  
180 (WML), and water vapor self-continuum (WCS), respectively. Note that the contribution of Rayleigh  
181 scattering is negligible. The cross-section  $C_S$ , expressed in cm<sup>2</sup>molecule<sup>-1</sup>atm<sup>-1</sup>, is defined by  $\alpha_{WCS} =$   
182  $\frac{1}{kT} C_S(\nu, T) P_{H_2O}^2$ , where  $k$  is the Boltzmann constant and  $P_{H_2O}$  is the water vapor pressure.

#### 183 a. Data analysis

184 The absorption due to the monomer lines was subtracted using the line-by-line fitting program MATS  
185 [27]. The water vapor transitions, as well as a few formaldehyde lines which were visible in the  
186 spectrum, were modeled from HITRAN2016 [28] parameters by Voigt profiles truncated at  $\pm 25$  cm<sup>-1</sup>  
187 from the line center. The formaldehyde concentration was fitted and estimated to be on the order of 10  
188 ppb. The HDO concentration was assumed to be 20 % lower than the natural abundance from HITRAN.  
189 The monomer-corrected values were averaged over a 0.3 cm<sup>-1</sup> wide part of the scan which is not much  
190 affected by the monomer lines (50 points near 2853.25 cm<sup>-1</sup>, shown in black in **Fig. 1**). The obtained  
191 data points are plotted in **Fig. 2** as a function of the squared pressure, with error bars corresponding to  
192 combined uncertainties including both statistical (type A) and type B uncertainties. Type B contributions  
193 to the uncertainty include the baseline uncertainty ( $2 \times 10^{-9}$  cm<sup>-1</sup>), and the uncertainty on the monomer  
194 lines, which is calculated by propagating the HITRAN error bars on the line intensities and self-  
195 broadening coefficients. Two simulations were performed, increasing either all intensities or all  $\gamma_{self}$   
196 values by their HITRAN error bars, yielding deviations from the usual HITRAN simulation which were  
197 then added in quadrature.

198 The slope of a linear regression yields the self-continuum cross-section  $C_S$ . The intercept of this  
199 regression corresponds to the empty-cavity losses  $\alpha_{cavity}$  and was subtracted in **Fig. 2**. The values given  
200 by the fit are reported here along with the fit uncertainty:  $5.85(42) \times 10^{-24}$  cm<sup>2</sup>molecule<sup>-1</sup>atm<sup>-1</sup> at 303 K,  
201  $4.28(39) \times 10^{-24}$  cm<sup>2</sup>molecule<sup>-1</sup>atm<sup>-1</sup> at 320 K.





202

203 **Figure 2:** Self-continuum absorption  $\alpha_{wcs}$  as a function of squared pressure, for two temperature values. The  
 204 self-continuum cross-section is obtained as the slope of the linear fits. The constant term due to the cavity losses,  
 205 obtained from the fit was subtracted, and shaded areas depict the fit uncertainty.

206

### b. Comparison to literature

207

208

209

210

211

212

213

214

215

216

217

218

219

220

221

222

223

224

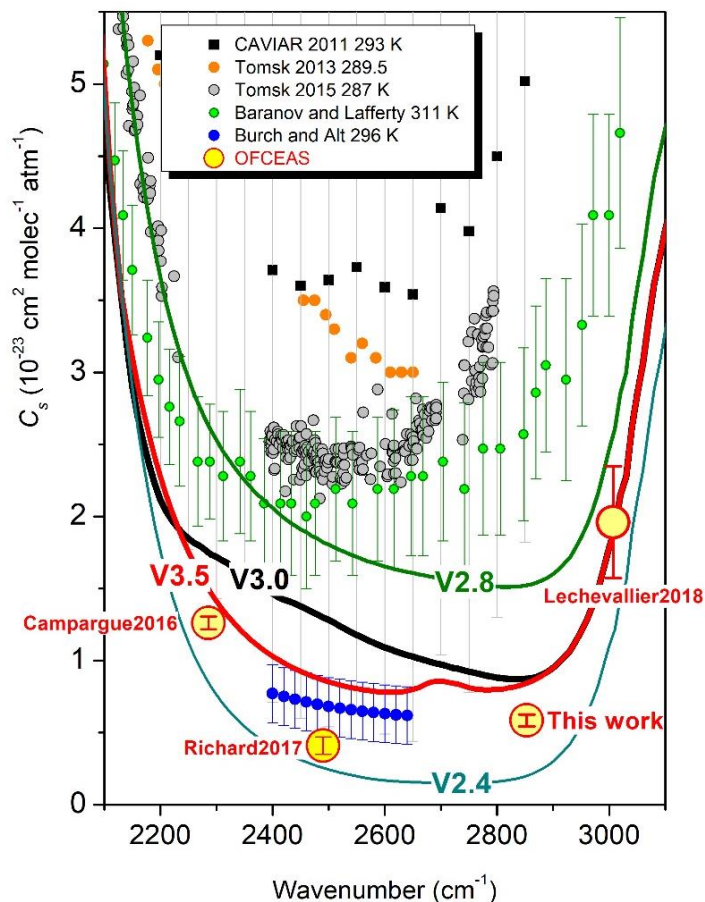
225

226

The different experimental determinations of the self-continuum cross-sections near room temperature in the 4  $\mu\text{m}$  window are plotted in **Fig. 3** together with some recent versions of the MT\_CKD continuum up to the current 3.5 version. Four datasets using long-path absorption cells and covering most of the transparency window were published prior to our series of OFCEAS measurements. In 1984, Burch and Alt retrieved the continuum between 2400 and 2640  $\text{cm}^{-1}$  using a grating spectrograph and a pathlength of 707 m [5,6]. An optical configuration which allowed changing the number of passes through the absorption cell without perturbing the optical alignment was adopted to minimize the spectra baseline drifts. The three other studies were performed by FTS: (i) the CAVIAR consortium performed room temperature measurements at the Rutherford Appleton Laboratory with a 512.7 m pathlength [8], (ii) a similar FTS approach with a pathlength of 612 m at 289.5 and 287 K, was adopted at the Institute of Atmospheric Optics in Tomsk [9,10], (iii) finally, Baranov and Lafferty, from NIST, reported FTS measurements between 311 and 363 K with a 100 m pathlength [29].

The OFCEAS measurements are limited by the availability of diode laser sources. Previous OFCEAS studies were performed at 2283  $\text{cm}^{-1}$  [13], 2491  $\text{cm}^{-1}$  [14] and 3007  $\text{cm}^{-1}$  [15] (see **Table 1**). The present measurement at 2853  $\text{cm}^{-1}$  completes the sampling of the window and is found consistent with previous OFCEAS values. The comparison to the FTS values is similar to that encountered in most of the transparency windows: although reported with large error bars, the FTS values are significantly larger than the laser measurements. Strictly speaking, only CAVIAR [8] and NIST [29] measurements are available for comparison near 2850  $\text{cm}^{-1}$ , Tomsk measurements [9,10] showing a gap in the 2800-3050  $\text{cm}^{-1}$  interval. Although the CAVIAR and NIST  $C_s$  values of  $5.0(3.2)\times 10^{-23}$  and  $2.6(6)\times 10^{-23}$

227  $\text{cm}^2\text{molecule}^{-1}\text{atm}^{-1}$  were reported with 65% and 23% error bars, respectively, the OFCEAS value of  
 228  $5.85(42)\times 10^{-24} \text{ cm}^2\text{molecule}^{-1}\text{atm}^{-1}$  falls outside the  $(1\sigma)$  FTS error bars.



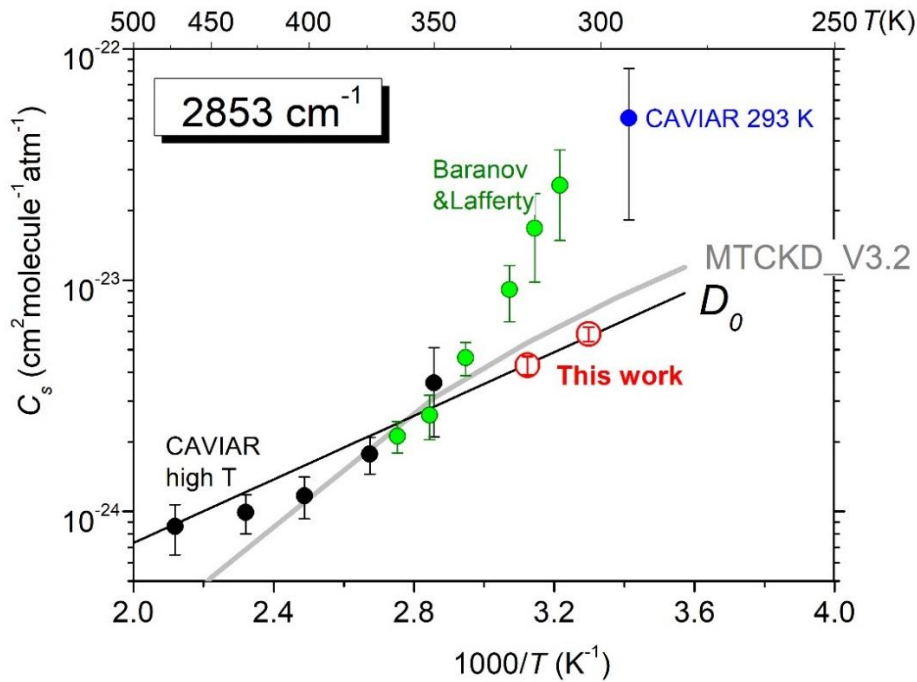
229  
 230 **Figure 3:** Overview comparison of the self-continuum cross-section of water vapor near room temperature in the  
 231  $4.0 \mu\text{m}$  window. Solid lines show different versions of the MT\_CKD model at 296 K [2-4]. Experimental results  
 232 were obtained by OFCEAS, (red circles; Campargue et al. [13]; Richard et al. [14]; Lechevallier et al. [15]; this  
 233 work); by FTS from Baranov and Lafferty [29] (light green circles), from CAVIAR (black squares; Ptashnik et  
 234 al. [8]), from Tomsk2013 (orange circles; Ptashnik et al. [9]), from Tomsk2015 (green circles; Ptashnik et al,  
 235 [10]) and with a grating spectrograph by Burch and Alt [5,6] (dark blue circles). Note that the plotted  
 236 experimental results correspond to different temperature values (see values given in the insert). The temperature  
 237 of the OFCEAS results are 296.15, 297.3, 298.15, and 303.15 K, for Campargue et al. [13]; Richard et al. [14];  
 238 Lechevallier et al. [15], and this work, respectively. The 30-50 % error bars on Tomsk2013 and Tomsk2015 values  
 239 are not plotted for clarity.

240  
 241 Over the last ten years, the different versions of the MT\_CKD model in the center of the  $4.0 \mu\text{m}$  window  
 242 varied over one order of magnitude (**Fig. 3**). On the basis of the OFCEAS measurement at  $2283 \text{ cm}^{-1}$   
 243 [13], the MT\_CKD 3.5 version of the self-continuum has been recently decreased in the low energy  
 244 edge of the window. At the  $2853 \text{ cm}^{-1}$  point of present interest, the MT\_CKD\_V3.5  $C_S$  value ( $8.73 \times 10^{-24}$   
 245  $\text{cm}^2\text{molecule}^{-1}\text{atm}^{-1}$ ) is larger than the OFCEAS value by about 50 %. Similar and even more  
 246 pronounced overestimation was noted at the  $2490 \text{ cm}^{-1}$  spectral point [14], indicating that in the very  
 247 center of the window, the MT\_CKD\_V3.5  $C_S$  values should be significantly decreased. It is interesting  
 248 to note that the pioneer results of Burch and Alt in the  $2400\text{-}2640 \text{ cm}^{-1}$  are the only previous  
 249 measurements in reasonable agreement with OFCEAS values in this region.

250 **c. Temperature dependence**

251 Atmospheric modeling requires the knowledge of the temperature dependence of the water vapor self-  
 252 continuum in particular at room temperature and below. Although the water self-continuum cross-  
 253 section is decreasing rapidly with temperature (about 36% for a temperature variation of 17 K presently  
 254 measured at 2853 cm<sup>-1</sup>), it is easier to measure the continuum at high temperature where larger saturation  
 255 pressures allow for increasing considerably the water vapor pressure. For instance, the CAVIAR  
 256 consortium reported measurements at temperatures from 350 to 472 K using a short-path absorption cell  
 257 and vapor pressure values up to 1.6 atm [8]. We have collected in **Fig. 4**, the  $C_S$  values available in the  
 258 literature at different temperatures around our measurement points at 2853 cm<sup>-1</sup> and plotted them in  
 259 logarithmic scale *versus* 1/T. In addition to the CAVIAR room and high temperature measurements, the  
 260 NIST data [29] cover the 311-363 K range.

261 The overall distribution of the experimental  $C_S$  values is very similar to what was observed at several  
 262 spectral points of the 4.0 and 2.1 μm windows (see Fig.7 of Ref. [15], Fig.6 of Ref. [14], Fig. 6 of Ref.  
 263 [18]), our two present  $C_S$  values are on line with the high temperature CAVIAR values while CAVIAR  
 264 room temperature value (obtained with a different FTS cell) is strongly overestimated. As already noted  
 265 for other spectral points, the OFCEAS and the CAVIAR high temperature values follow a simple  
 266 exponential law in 1/T with a slope close to the dissociation energy of the water dimer,  $D_0 \approx 1100$  cm<sup>-1</sup>  
 267 [30].



268  
 269 **Figure 4:** Temperature dependence of the water vapor self-continuum cross-sections near 2853 cm<sup>-1</sup> obtained by  
 270 OFCEAS (open red circles), by FTS (CAVIAR at high temperature [8] (green squares): CAVIAR at room  
 271 temperature [8] (full blue circle): Baranov and Lafferty [29] (full green circles). The MT\_CKD\_V3.5 values which  
 272 are normalized to the number density at 1 atm and 296 K were multiplied by 296/T. The  $D_0$  slope corresponds to  
 273 an  $\exp(D_0/kT)$  function,  $D_0 \approx 1100$  cm<sup>-1</sup> being the dissociation energy of the water dimer molecule.  
 274

275 The MT\_CKD\_V3.5 temperature dependence at 2853 cm<sup>-1</sup> included in **Fig. 4** shows a behavior close to  
 276 the  $\exp\left(\frac{D_0}{kT}\right)$  function near room temperature while at higher temperature, the MT\_CKD self-continuum  
 277 is decreasing more rapidly than observed from the high temperature CAVIAR measurements.

#### 278 4. Foreign continuum at 4302 cm<sup>-1</sup>

279 As mentioned above, the foreign-continuum measurements were performed at a constant total pressure  
 280 of 510 Torr, for two temperature values (34°C and 47°C) and four water mole fraction values of 5000,  
 281 10000, 12500 and 15000 ppmv.

282 In a mixture of water vapor in air, the total absorption coefficient can be expressed as the sum of four  
 283 terms:

$$284 \quad \alpha_{tot}(\nu, T) = \alpha_{cavity} + \alpha_{WML} + \alpha_{WCS} + \alpha_{WCF}$$

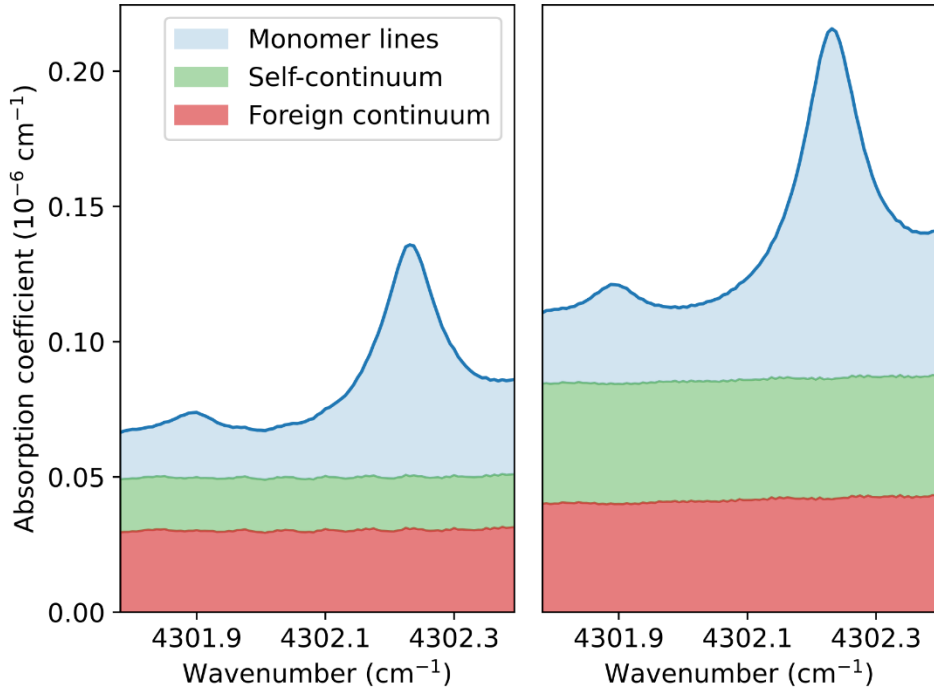
$$285 \quad = \alpha_{cavity} + \alpha_{WML} + \frac{1}{kT} C_S(\nu, T) P_{H_2O}^2 + \frac{1}{kT} C_F(\nu, T) P_{H_2O} P_{air} \quad (3)$$

286 where, in comparison to Eq. (2), the additional term  $\alpha_{WCF}$  denotes the contribution due to the foreign-  
 287 continuum (WCF), with  $C_F$  expressed in cm<sup>2</sup>molecule<sup>-1</sup>atm<sup>-1</sup>.  $P_{H_2O}$  and  $P_{air}$  are the water vapor and dry  
 288 air partial pressures, respectively. Due to the negligible difference ( $\sim 10^{-11}$  cm<sup>-1</sup>) in Rayleigh scattering  
 289 losses between the pure nitrogen baseline measurements and the moist air measurements at the same  
 290 pressure, the Rayleigh contribution was omitted from Eq. (3).

##### 291 a. Data analysis

292 In a first step, the baseline absorption  $\alpha_{cavity}$ , measured while flowing the cavity with pure N<sub>2</sub> at the  
 293 same nominal pressure as the water mixture measurements (510 Torr), was subtracted from each  
 294 spectrum. **Figure 5** shows the various contributions to the remaining absorption for two values of the  
 295 water vapor molar fraction. The absorption due to the water monomer lines was calculated from  
 296 HITRAN2016 parameters using Voigt profiles truncated at  $\pm 25$  cm<sup>-1</sup> from the line center without  
 297 including the pedestal. The isotopic abundance of HDO was reduced by 20% as compared to the  
 298 HITRAN natural abundance. There were no observable lines from other species.

299 In this spectral region the self-continuum cross-section has been measured in a previous work [18], over  
 300 a temperature range comprising the temperatures studied here. We interpolated the reported  $C_S$  values  
 301 from Ref. [18] to calculate the self-continuum absorption at our experimental conditions ( $C_S$  values of  
 302  $1.88 \times 10^{-23}$  and  $1.55 \times 10^{-23}$  cm<sup>2</sup> molecule<sup>-1</sup> atm<sup>-1</sup> were used at 34 °C and 47 °C, respectively). Obviously,  
 303 the total pressure being identical, the relative contribution of the self-continuum is larger for the higher  
 304 mole fractions (see **Fig. 5**).



305

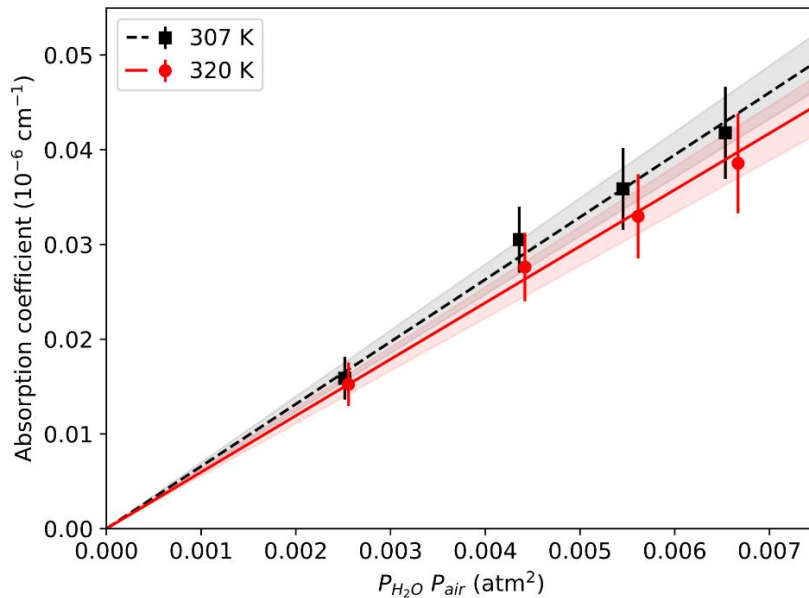
306 **Figure 5:** Baseline-corrected spectra recorded for two water vapor molar fractions (left: 10 000 ppmv, right:  
 307 15 000 ppmv), at a temperature of 307 K. The total pressure was 510 Torr. The shaded areas show the absorption  
 308 due to local monomer lines (in blue), the self-continuum (in green) and the foreign continuum (in red). Note that  
 309 the self-continuum absorption grows faster than the other two contributions with the water vapor molar fraction,  
 310 reflecting its quadratic dependence on water vapor density.

311 Type B uncertainties were calculated from Eq. (3) by error propagation. The uncertainty on the baseline  
 312 absorption  $\alpha_{cavity}$  is taken to be  $1 \times 10^{-9} \text{ cm}^{-1}$ , while a 2% uncertainty is estimated for the water vapor  
 313 pressure determined from the hygrometer reading. The monomer contribution uncertainty was  
 314 determined by propagating the HITRAN error bars of the line intensities, self-broadening and air-  
 315 broadening coefficients, as well as the water vapor partial pressure uncertainty. Four simulations were  
 316 performed, each of them with either the intensities,  $\gamma_{self}$ ,  $\gamma_{air}$  coefficients or  $P_{H_2O}$  values increased by their  
 317 error bar, yielding deviations  $\delta_i(\nu)$  from the usual HITRAN simulation. The uncertainty on  $\alpha_{WML}$  was  
 318 obtained as  $\delta\alpha_{WML}(\nu) = [\sum_{i=1}^4 \delta_i(\nu)^2]^{1/2}$ . The  $C_s$  uncertainty was taken from Ref. [18].

319 The values of  $\alpha_{WCF}$  were averaged over the extent of the  $0.6 \text{ cm}^{-1}$  wavenumber range of each scan. The  
 320 average values are plotted in **Fig. 6** as a function of the product of the water vapor pressure  $P_{H_2O}$  and air  
 321 pressure  $P_{air}$ . The error bars on this plot show the combined uncertainty including both the statistical  
 322 (type A) uncertainty given by the standard deviation of the averaged spectral points, and the type B  
 323 uncertainty described above.

324 The slope of a linear fit, weighted by the inverse of the variance of each point, gives the foreign  
 325 continuum cross-section  $C_F$ . The values derived from the fits are reported here along with the fit  
 326 uncertainty:  $2.75(17) \times 10^{-25} \text{ cm}^2 \text{ molecule}^{-1} \text{ atm}^{-1}$  at 307 K,  $2.60(18) \times 10^{-25} \text{ cm}^2 \text{ molecule}^{-1} \text{ atm}^{-1}$  at 320 K.  
 327 The small temperature difference of 13 K between our two series of measurements does not allow to

328 evidence a significant variation and we can merely confirm that the foreign-continuum has a small  
 329 temperature dependence.



330

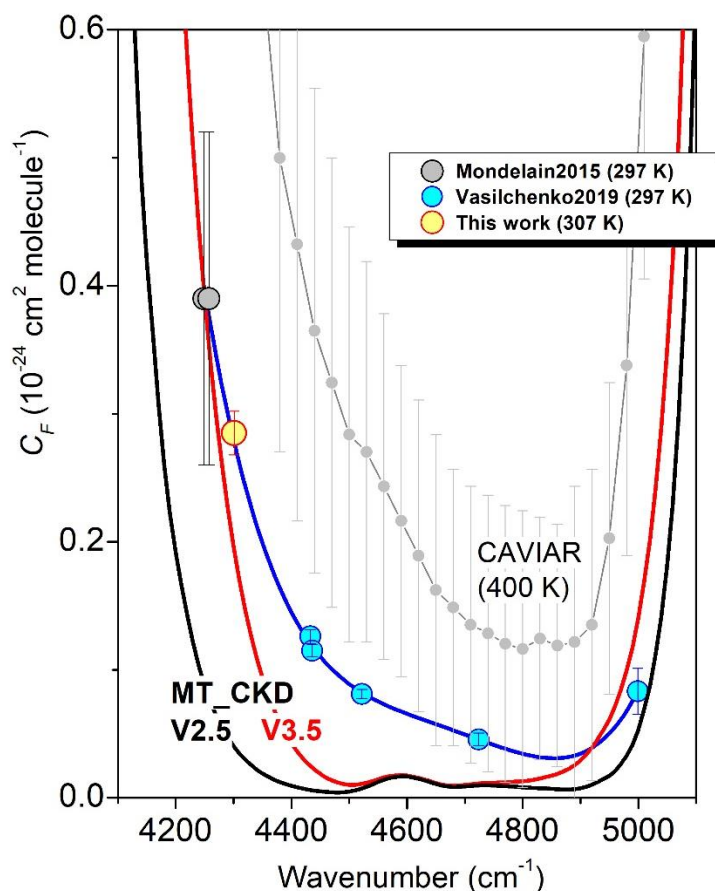
331 **Figure 6:** Foreign continuum absorption  $\alpha_{WCF}$  as a function of the product of water vapor and air pressures, for  
 332 two temperature values. The error bars shown here correspond to the combined uncertainty including both type  
 333 A and type B uncertainties. The slopes of linear fits, also plotted, give the foreign continuum cross-sections  $C_F$ .  
 334 Shaded areas show the uncertainty on the fitted slopes.

335 **b. Comparison to literature**

336 The comparison of the available experimental determination of the foreign-continuum cross-sections in  
 337 the 2.1  $\mu\text{m}$  window to the MT\_CKD\_V3.5 values is presented in **Fig. 7**. Experimental data at room  
 338 temperature are limited to the present OFCEAS determination at 4310  $\text{cm}^{-1}$ , the CRDS data points at  
 339 4250  $\text{cm}^{-1}$  [16] and at 4433, 4436, 4522, 4724 and 4999  $\text{cm}^{-1}$  [17]. The CAVIAR consortium reported  
 340 foreign-continuum absorption by FTS between 1.1 and 5  $\mu\text{m}$  at high temperatures (350-431 K) with an  
 341 absorption path length of 17.7 m [31]. The chosen elevated temperatures allowed for increasing the  
 342 water vapor partial pressure of the recordings between 266 and 600 mbar. Compared to our measurement  
 343 conditions, these high water vapor pressure values combined with air pressure of about 4 atm led to an  
 344 increase of the foreign-continuum absorption signal by two or three orders of magnitude. The FTS  
 345 recordings between 350 and 431 K did not reveal temperature dependence greater than the uncertainty  
 346 in those measurements. The  $C_F$  values included in **Fig. 7** are those reported by Ptashnik et al. at the 400  
 347 K average temperature [31].

348 The CRDS and OFCEAS  $C_F$  cross-sections values represent a consistent dataset which can be  
 349 reproduced by a 4<sup>th</sup> order polynomial fit (see Fig. 7) - the corresponding polynomial coefficients are  
 350 given in the figure caption.

351 Overall the present OFCEAS and previous CRDS room temperature  $C_F$  values are systematically below  
 352 the CAVIAR values (at 400 K) by a factor between 2 and 4. In the center of the window, the FTS relative  
 353 uncertainties are very large (up to 93 %) which makes the CRDS value at 4724  $\text{cm}^{-1}$  fall within the  
 354  $1\sigma$  FTS confidence interval. This is not the case on the low energy edge of the window. For instance at  
 355 the 4302  $\text{cm}^{-1}$  spectral point presently measured, CAVIAR  $C_F$  value is  $5.8(2.2)\times 10^{-25} \text{cm}^2 \text{molecule}^{-1} \text{atm}^{-1}$   
 356 to be compared to an OFCEAS value of  $2.75(6)\times 10^{-25} \text{cm}^2 \text{molecule}^{-1} \text{atm}^{-1}$  at 307 K (the corresponding  
 357 density normalized  $C_F$  values are 7.8(3.0) and 2.85(6)  $\text{cm}^2 \text{molecule}^{-1} \text{atm}^{-1}$ ). If the CAVIAR values at  
 358 400 K are confirmed, it would indicate that the foreign-continuum exhibits significant *positive*  
 359 temperature dependence.

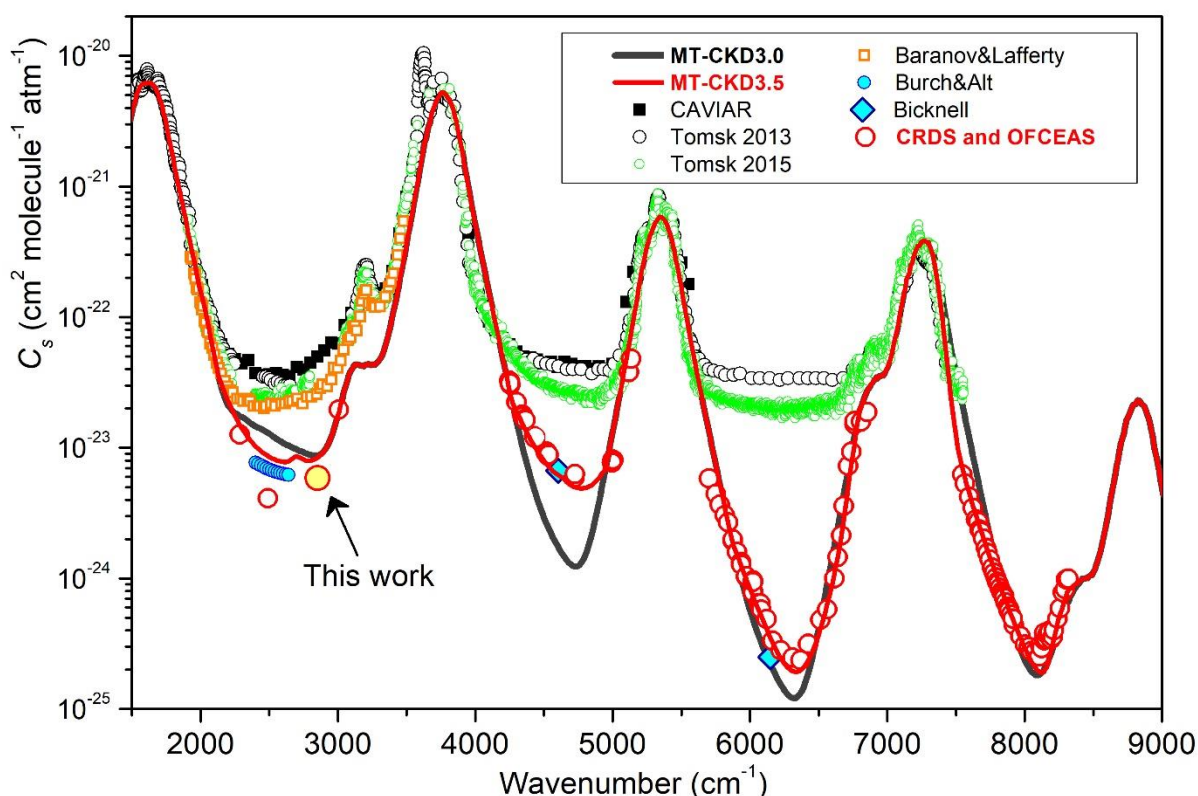


360  
 361 **Figure 7.** Overview of the experimental foreign-continuum cross-sections,  $C_F$ , reported in the literature and  
 362 retrieved in this work (red circle) for the 2.1  $\mu\text{m}$  window and comparison to the MT\_CKD model in its versions  
 363 3.5 (red) and 2.5 (black). Previous experimental determinations are the CAVIAR FTS values at 400 K from Ref.  
 364 [31] (full grey circles) and the CRDS values (light blue circles) from Vasilchenko et al. [16] at 4250  $\text{cm}^{-1}$ ) and  
 365 from Mondelain et al. [17] at 4433, 4436, 4522, 4724, 4999  $\text{cm}^{-1}$ . Note that for comparison purposes, the  $C_F$  values  
 366 are density normalized and are given in  $\text{cm}^2 \text{molecule}^{-1}$  (density normalized  $C_F$  values in  $\text{cm}^2 \text{molecule}^{-1}$  correspond  
 367 to  $C_F$  values in  $\text{cm}^2 \text{molecule}^{-1} \text{atm}^{-1}$  multiplied by the factor  $T/296$ ). The blue solid line corresponds to the fit of  
 368 the CRDS and OFCEAS data with a 4<sup>th</sup> order polynomial:  $3.99039496\times 10^{-21}-3.41093025\times 10^{-24}v+1.09342553\times 10^{-27}v^2-1.55784737\times 10^{-31}v^3+8.32287078\times 10^{-36}v^4$  where  $v$  is the wavenumber in  $\text{cm}^{-1}$ .  
 369

370 The MT\_CKD\_V3.5 foreign-continuum included in **Fig. 7** is assumed to be temperature independent.  
 371 The MT\_CKD foreign-continuum was recently increased in the 2.1  $\mu\text{m}$  window, taking into account our  
 372 CRDS value at 4250  $\text{cm}^{-1}$  [17] and the NIST values [29] in the 4.0  $\mu\text{m}$  window (the MT\_CKD\_2.5 is

373 included in **Fig. 7**, for comparison). On the low and high energy range of the window, the agreement  
 374 with CRDS and OFCEAS values has become reasonable but the MT\_CKD foreign-continuum should  
 375 be significantly increased in the centre of the window (by a factor of about 5 for the minimum  $C_F$  values  
 376 near  $4700\text{ cm}^{-1}$ ).

### 377 5. Conclusion



378  
 379 **Figure 8:** Overview comparison of the self-continuum cross-section of water vapor near room temperature  
 380 between  $1500$  and  $9000\text{ cm}^{-1}$ .

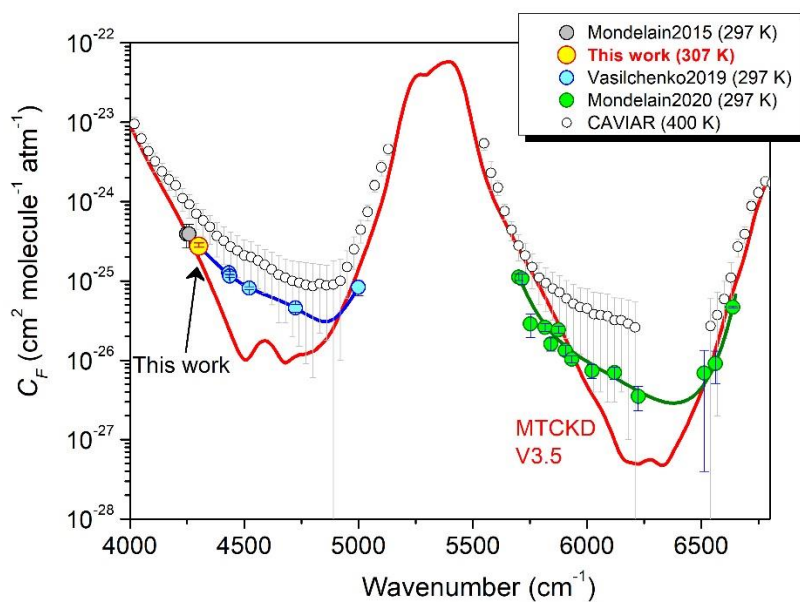
381 Solid lines show different versions of the MT\_CKD V3.0 and V3.5 versions at  $296\text{ K}$  [2-4]. Experimental results  
 382 were obtained by OFCEAS and CRDS (red circles; Campargue et al. [13], Richard et al. [14], Lechevallier et al.  
 383 [15], Ventrillard et al. [18], Mondelain et al. [16], Vasilchenko et al. [17] and this work); by FTS from Baranov  
 384 and Lafferty [29]) (light green circles), from CAVIAR consortium (black squares; Ptashnik et al. [8]), from  
 385 Tomsk2013 (orange circles; Ptashnik et al. [9]), from Tomsk2015 (green circles; Ptashnik et al. [10]), with a  
 386 grating spectrograph by Burch and Alt [5,6] (dark blue circles) and by interferometric calorimetry (blue diamond;  
 387 Bicknell et al. [32]).

388  
 389 The present measurements of the self-continuum cross-section of water vapor at  $2853\text{ cm}^{-1}$  and  
 390 of the foreign-continuum cross-sections at  $4302\text{ cm}^{-1}$  complete the previous CEAS characterizations of  
 391 the water vapor continuum absorption that we performed in the  $4.0$ ,  $2.1$ ,  $1.6$  and  $1.25\text{ }\mu\text{m}$  windows. **Figs.**  
 392 **8** and **9** present an updated overview comparison of our measured  $C_S$  and  $C_F$  values to the MT\_CKD  
 393 model and to previous FTS measurements. The consistency of our measurements performed since 2013  
 394 by different experimentators, with two different CEAS techniques (CRDS and CEAS) using a large  
 395 variety of spectrometers covering very different spectral regions, has to be underlined. It is now admitted



396 that the FTS self-continuum values reported by the CAVIAR consortium at room temperature are largely  
 397 overestimated in the windows because they were affected by experimental biases. The current version  
 398 of the MT\_CKD self-continuum has been recently constrained according to most of the CEAS cross-  
 399 sections in the 4.0, 2.1, 1.6 and 1.25  $\mu\text{m}$  windows. The present  $C_S$  measurement at  $2853\text{ cm}^{-1}$  together  
 400 with the previous OFCEAS measurement at the  $2490\text{ cm}^{-1}$  spectral point [14], indicate the  
 401 MT\_CKD\_V3.5 self-continuum values should be significantly decreased in the center of the 4.0  $\mu\text{m}$   
 402 window.

403 As concerns the foreign continuum, to the best of our knowledge no room temperature  
 404 measurements were available prior to our OFCEAS and CRDS investigations. The overview comparison  
 405 of **Fig. 9** indicates that the MT\_CKD\_V3.5 foreign-continuum is significantly smaller than the  
 406 observations near the center of the 1.6 and 2.1  $\mu\text{m}$  windows. The two sets of CEAS measurements can  
 407 be satisfactorily reproduced using a polynomial which is given above for the 2.1  $\mu\text{m}$  window (see  
 408 caption of Fig. 7) and can be found in Ref. [19] for the 1.6  $\mu\text{m}$  window. The CAVIAR FTS  $C_F$  values  
 409 at 400 K [31] are larger than the room temperature CEAS values. However, the data at disposal do not  
 410 allow for a conclusive statement about the temperature dependence of the foreign continuum. In the near  
 411 future, we plan to investigate this issue in more details using a newly developed CRDS cell allowing for  
 412 measurements over a wider temperature range than allowed by our OFCEAS spectrometers.



413  
 414 **Figure 9.** Overview of the experimental foreign-continuum cross-sections,  $C_F$ , reported in the literature and  
 415 retrieved in this work (red circle) for the 2.1 and 1.6  $\mu\text{m}$  windows and comparison to the MT\_CKD\_V3.5 model  
 416 (red solid line). Previous experimental determinations are the CAVIAR FTS values at 400 K from Ref. [31] (black  
 417 circles), CRDS values (light blue circles) from Vasilchenko et al. [16] at  $4250\text{ cm}^{-1}$ , from Mondelain et al. [17] at  
 418  $4433, 4436, 4522, 4724, 4999\text{ cm}^{-1}$  and from Mondelain et al. [19] in the 1.6  $\mu\text{m}$  window.

#### 419 Acknowledgements

420 This work was performed in the frame of the ANR project COMPLEAT (ANR-19-CE31-0010-01).

- 422 1. Shine KP, Campargue A, Mondelain D, McPheat RA, Ptashnik IV, Weidmann D. The water  
423 vapor continuum in near-infrared windows – Current understanding and prospects for its  
424 inclusion in spectroscopic databases. *J Molec Spec* 2016;327:193–208. doi:  
425 10.1016/j.jms.2016.04.011
- 426 2. Clough SA, Kneizys FX, Davies RW. Line shape and the water vapor continuum. *Atm Res*  
427 1989;23:229-241. doi:10.1016/0169-8095(89)90020-3
- 428 3. Mlawer EJ, Payne VH, Moncet J, Delamere JS, Alvarado MJ, Tobin DC. Development and  
429 recent evaluation of the MT\_CKD model of continuum absorption. *Phil Trans R Soc A*  
430 2012;370:2520–2556. doi:10.1098/rsta.2011.0295
- 431 4. [http://rtweb.aer.com/continuum\\_description.html](http://rtweb.aer.com/continuum_description.html)
- 432 5. Burch DE. Continuum absorption by H<sub>2</sub>O. Report AFGL-TR-81-0300, Air Force Geophys.  
433 Laboratory, Hanscom AFB, MA, 1982.
- 434 6. Burch DE, Alt RL. Continuum absorption by H<sub>2</sub>O in the 700 – 1200 cm<sup>-1</sup> and 2400 – 2800 cm<sup>-1</sup>  
435 windows. Report AFGL-TR-84-0128, Air Force Geophys. Laboratory, Hanscom AFB, MA,  
436 1984.
- 437 7. Burch DE. Absorption by H<sub>2</sub>O in narrow windows between 3000 and 4200 cm<sup>-1</sup>. Report AFGL-  
438 TR-85-0036, Air Force Geophys. Laboratory, Hanscom AFB, MA, 1985.
- 439 8. Ptashnik IV, McPheat RA, Shine KP, Smith KM, Williams RG. Water vapor self-continuum  
440 absorption in near-infrared windows derived from laboratory measurements. *J Geophys Res*  
441 2011;116: D16305. doi:10.1029/2011JD015603
- 442 9. Ptashnik IV, Petrova TM, Ponomarev YN, Shine KP, Solodov AA, Solodov AM. Near-infrared  
443 water vapor self-continuum at close to room temperature. *J Quant Spectrosc Radiat Transfer*  
444 2013;120:23–35. doi:10.1016/j.jqsrt.2013.02.016
- 445 10. Ptashnik IV, Petrova TM, Ponomarev YN, Solodov AA, Solodov AM. Water vapor continuum  
446 absorption in near-IR atmospheric windows. *Atmos Oceanic Opt* 2015;28:115–120.  
447 doi:10.1134/S102485601502009
- 448 11. Mondelain D, Aradj A, Kassi S, Campargue A. The water vapor self-continuum by CRDS at  
449 room temperature in the 1.6 μm transparency window. *J Quant Spectrosc Radiat Transfer*  
450 2013;130:381–91. doi: 10.1016/j.jqsrt.2013.07.006.
- 451 12. Mondelain D, Manigand S, Manigand S, Kassi S, Campargue A. Temperature de-  
452 pendence of the water vapor self-continuum by cavity ring-down spectroscopy in the 1.6 μm transparency  
453 window. *J Geophys Res Atmos* 2014;119(9):2169–8996. doi: 10.1002/2013JD021319.
- 454 13. Campargue A, Kassi S, Mondelain D, Vasilchenko S, Romanini D. Accurate laboratory  
455 determination of the near infrared water vapor self-continuum: A test of the MT\_CKD model.  
456 *J Geophys Res Atmos* 2016;121:13,180 – 13,203. doi:10.1002/2016JD025531
- 457 14. Richard L, Vasilchenko S, Mondelain D, Ventrillard I, Romanini D, Campargue A. Water vapor  
458 self-continuum absorption measurements in the 4.0 and 2.1 μm transparency windows. *J Quant*  
459 *Spectrosc Radiat Transf* 2017;201:171–179. doi: 10.1016/j.jqsrt.2017.06.037
- 460 15. Lechevallier L, Vasilchenko S, Grilli R, Mondelain D, Romanini D, Campargue A. The water  
461 vapor self-continuum absorption in the infrared atmospheric windows: new laser measurements  
462 near 3.3 and 2.0 μm. *Atmos Meas Tech* 2018;11:2159–2171. doi:10.5194/amt-11-2159-2018
- 463 16. Mondelain D, Vasilchenko S, Čermák P, Kassi S, Campargue A. The self- and foreign-  
464 absorption continua of water vapor by cavity ring-down spectroscopy near 2.35 μm. *Phys Chem*  
465 *Chem Phys* 2015;17:17,762–17,770. doi: 10.1039/c5cp01238d
- 466 17. Vasilchenko S, Campargue A, Kassi S, Mondelain D. The water vapor self- and foreign-  
467 continua in the 1.6 μm and 2.3 μm windows by CRDS at room temperature. *J Quant Spectrosc*  
468 *Radiat Transfer* 2019;227:230–238. doi: 10.1016/j.jqsrt.2019.02.01
- 469 18. Ventrillard I, Romanini D, Mondelain D, Campargue A. Accurate measurements and  
470 temperature dependence of the water vapor self-continuum absorption in the 2.1 μm  
471 atmospheric window. *J Chem Phys* 2015;143:134304. doi: 10.1063/1.4931811]
- 472 19. Mondelain D, Vasilchenko S, Kassi S, Campargue A. The water vapor foreign-continuum in the  
473 1.6 μm window by CRDS at room temperature *J. Quant. Spectrosc. Radiat. Transfer* 246 (2020)  
474 106923 doi.org/10.1016/j.jqsrt.2020.106923

- 475 20. Hartmann J-M, Tran H, Armante R, Boulet C, Campargue A, Forget F, Gianfrani L, Gordon I,  
476 Guerlet S, Gustafsson M, Hodges JT, Kassı S, Lisak D, Thibault F, Toon GC. Recent advances  
477 in collisional effects on spectra of molecular gases and their practical consequences, *J Quant*  
478 *Spectrosc Radiat Transfer* 2018;213:178–227. doi: 10.1016/j.jqsrt.2018.03.016
- 479 21. Baranov YI. The continuum absorption in H<sub>2</sub>O+N<sub>2</sub> mixtures in the 2000–3250 cm<sup>-1</sup> spectral  
480 region at temperatures from 326 to 363 K. *J Quant Spectrosc Radiat Transfer* 2011;112:2281–  
481 2286. doi:10.1016/j.jqsrt.2011.06.005
- 482 22. Baranov YI, Buryak IA, Lokshantov SE, Lukyanchenko VA, Vigasin AA. H<sub>2</sub>O–N<sub>2</sub> collision-  
483 induced absorption band intensity in the region of the N<sub>2</sub> fundamental: ab initio investigation of  
484 its temperature dependence and comparison with laboratory data. *Phil Trans R Soc A*  
485 2012;370:2691–2709. doi: 10.1098/rsta.2011.0189.
- 486 23. Baranov YI and Lafferty WJ. The water vapor self- and water-nitrogen continuum absorption in  
487 the 1000 and 2500 cm<sup>-1</sup> atmospheric windows. *Phil Trans R Soc A* 2012;370:2578–2589. doi:  
488 10.1098/rsta.2011.0234
- 489 24. Morville, J., Romanini, D., Kachanov, A. A., Chenevier M.: Two schemes for trace detection  
490 using cavity ringdown spectroscopy, *Appl. Phys.*, 78, 465–476, doi:10.1007/s00340-003-1363-  
491 8, 2004.
- 492 25. Romanini, D., Chenevier, M., Kassı, S., Schmidt, M., Valant, C., Ramonet, M., Lopez, J., and  
493 Jost, H. J.: Optical-feedback cavity-enhanced absorption: a compact spectrometer for real-time  
494 measurement of atmospheric methane, *App. Phys. B-Lasers and Optics.*, 83, 659-667,  
495 doi:10.1007/s00340-006-2177-2, 2006.
- 496 26. Kerstel, E., Iannone, R. Q., Chenevier, M., Kassı, S., Jost, H. J., and Romanini, D.: A water  
497 isotope (<sup>2</sup>H, <sup>17</sup>O, and <sup>18</sup>O) spectrometer based on optical feedback cavity-enhanced absorption  
498 for in situ airborne applications, *Applied Physics B-Lasers and Optics*, 85, 397-406.  
499 doi:10.1007/s00340-006-2356-1, 2006.
- 500 27. Adkins EM, 2020. doi:10.18434/M32200
- 501 28. Gordon IE, Rothman LS, Hill C, Kochanov RV, Tan Y, Bernath PF, Birk M, Boudon V,  
502 Campargue A, Chance KV, Drouin BJ, Flaud JM, Gamache RR, Hodges JT, Jacquemart D,  
503 Perevalov, VI, Perrin A, Shine KP, Smith MAH, Tennyson J, Toon GC, Tran H, Tyuterev VG,  
504 Barbe A, Császár, AG, Devi VM, Furtenbacher T, Harrison JJ, Hartmann J-M, Jolly A, Johnson  
505 TJ, Karman T, Kleiner, I, Kyuberis AA, Loos J, Lyulin OM, Massie ST, Mikhailenko SN,  
506 Moazzen-Ahmadi N, Müller HSP, Naumenko OV, Nikitin AV, Polyansky OL, Rey M, Rotger  
507 M, Sharpe SW, Sung K, Starikova E, Tashkun SA, Vander Auwera J, Wagner G, Wilzewski J,  
508 Weisłó P, Yu S, Zak EJ. The HITRAN2016 Molecular Spectroscopic Database. *J Quant*  
509 *Spectrosc Radiat Transf* 2017;203:3-69. doi: 10.1016/j.jqsrt.2017.06.038
- 510 29. Baranov YI and Lafferty WJ. The water vapor self- and water-nitrogen continuum absorption in  
511 the 1000 and 2500 cm<sup>-1</sup> atmospheric windows. *Phil Trans R Soc A* 2012;370:2578–2589. doi:  
512 10.1098/rsta.2011.0234
- 513 30. Rocher-Casterline BE, Ch'ng LC, Mollner AK, Reisler H. Determination of the bond  
514 dissociation energy (D<sub>0</sub>) of the water dimer, (H<sub>2</sub>O)<sub>2</sub>, by velocity map imaging, *Chem, J.:Phys.*,  
515 134, 211101, 2011.
- 516 31. Ptashnik IV, McPheat RA, Shine KP, Smith KM, Williams RG. Water vapor foreign-continuum  
517 absorption in near-infrared windows from laboratory measurements. *Phil Trans R Soc A*  
518 2012;370: 2557–2577. doi:10.1098/rsta.2011.0218
- 519 32. Bicknell WE, Cecca SD, Griffin MK. Search for low-absorption regions in the 1.6- and 2.1- $\mu$ m  
520 atmospheric windows. *J Directed Energy* 2006;2:151–61.